

SYNTHESIS AND CHARACTERIZATION OF COPPER OXIDE NANOSTRUCTURES FOR SUPERCAPACITOR ELECTRODE APPLICATIONS

R. SURESH^{a*}, K. TAMILARASAN^b, D. S. VADIVU^c

^a*Department of Physics, Sri Eshwar College of Engineering, Kondampatti, Kinathukadavu, Coimbatore, Tamil Nadu, India- 641202*

^b*Department of Physics, Kongu Engineering College, Erode, Tamilnadu, India- 638 052*

^c*Department of Chemistry, Dr. Mahalingam College of Engineering and Technology, Pollachi, Tamilnadu, India- 642 003*

Facile and simple co-precipitation method has been used to synthesis copper oxide (CuO) nanostructures. The effect of temperature on the structural, morphological and electrochemical properties of the CuO has been studied and reported. X-ray diffraction pattern confirms the formation of monoclinic CuO at 300, 400 and 500°C. Electrochemical investigation indicates that the CuO nanostructures prepared at 400°C reveals a specific capacitance of 345 Fg⁻¹ at 2 mV s⁻¹. Cycle-life tests show that the capacitance retention of the CuO nanoworms is 99 % even after 1500 cycles. The lower charge transfer resistance (3.3 Ω) of this material enhances their supercapacitive features. Furthermore, an asymmetric supercapacitor device was constructed using CuO nanoworms and activated carbon (AC) as electrode materials. The functional performance of the system showed a specific capacitance of 47 Fg⁻¹ with an energy density/ power density of 6.5 Whkg⁻¹ and 249 Wkg⁻¹ respectively.

(Received June 19, 2016; Accepted August 4, 2016)

Keywords: Energy storage; supercapacitors; Nanostructures; Electrochemical properties

1. Introduction

Global warming, as well as the increasing price and decreasing availability of fossil fuels, all highlight the need to move towards a sustainable development, where it is critical to preserve the environment and to build highly efficient renewable energy storage/conversion systems. Supercapacitors, as a new class of energy storage device, are specialised form of capacitors with an exceedingly high level of capacitance. They have received significant attention in recent years because they can achieve higher energy density than conventional capacitors and offer better power performance than batteries [1, 2].

Based on the charge storage mechanism, supercapacitors are classified as electric double layer capacitors (EDLC) and pseudo-capacitors or ultracapacitors. EDLCs, which store charges electrostatically, through reversible ion adsorption at the electrode/electrolyte interface, commonly use carbon-based electrode materials with high surface area, high conductivity, electrochemical stability and open porosity. In contrast, pseudocapacitors are based on transition metal oxides (TMO) where charge storage occurs through electrochemical redox reactions [3-6]. Among the TMOs, RuO₂ has been widely investigated because of its high conductivity, remarkable specific capacitance and distinct oxidation states. Although RuO₂ can offer excellent charge storage performance, the high cost and toxicity of RuO₂ hinders its use in practical applications. More cost-effective transition metal oxides such as MnO₂, Fe₃O₄, V₂O₅, NiO etc., owing to their hallmark properties such as tuneable morphology, lesser toxicity and multiple valences are widely exploited towards supercapacitor electrode applications but the poor electronic conductivity of these oxides deters their use in high power applications. Nevertheless, nanostructures of these

*Corresponding author: suresh.r@sece.ac.in

metal oxides possess better electronic conductivity, higher specific capacitance and enhanced cycling stability [7,8].

Recently, CuO nanostructures have attracted considerable interest with regard to battery and bio-sensing applications due to their low cost and environmental friendly nature [9-11]. Synthesizing unique nanostructures of Cu oxides could mitigate poor cyclic stability and lower conductivity because nanostructures may endow additional pathways for electrolyte penetration and maintain the sustainability of the crystal structure during cycling.

Simple fabrication procedure and cost effectiveness of nanostructured materials are much favoured for mass production and commercialization. In this study, we report, a simple and inexpensive procedure based on precipitation technique to fabricate CuO nanostructures and studied their potential towards supercapacitor electrode applications.

2. Experimental section

2.1 Reagents and chemicals

Analytical grade copper nitrate ($\text{Cu}(\text{NO}_3)_2 \cdot 3\text{H}_2\text{O}$), sodium hydroxide (NaOH) and ethylene glycol were purchased from SD Fine Chemicals Ltd., India. Disodium citrate ($\text{Na}_2\text{HC}_6\text{H}_5\text{O}_7$) was obtained from Sigma Alrich, India. All reagents were utilized as such without further purification process.

2.2 Synthesis of CuO nanostructures

For the typical synthesis of CuO nanostructures, 1.8121 g of copper nitrate ($\text{Cu}(\text{NO}_3)_2 \cdot 3\text{H}_2\text{O}$) was dissolved in 250 mL of double distilled water (DI) under constant stirring. Then, 2 mL of ethylene glycol and 0.09g of disodium citrate was added to the solution followed by addition of 2M NaOH drop by drop to make the pH~10. Further, the solution is stirred for 5 hrs to produce homogenous mixture and aged for 2 days. With the help of centrifugation, the samples were collected and dried overnight at 80°C to get the final product. The as prepared samples were annealed at 300°C, 400°C and 500°C for two hours and are named as Cu3, Cu4 and Cu5 respectively.

2.3 Characterization of CuO nanostructures

The X-ray diffraction analysis were made from 10° to 80° using PANALYTICAL XPERT-PRO X-ray diffractometer with $\text{CuK}\alpha$ radiation to determine the phase and purity of the samples. The field emission scanning electron microscopy (FESEM) investigations were carried out using SEM FEI-Quanta FEG 200. Electrochemical investigations like cyclic voltammetry (CV), galvanostatic charge-discharge analysis and electrochemical impedance spectroscopy (EIS) measurements were performed using CHI 660 D electrochemical workstation (CH Instruments).

2.4 Fabrication of electrodes for supercapacitor applications

Electrochemical studies of CuO samples were performed using a three-electrode set up, consists of CuO nanostructures as working electrode, platinum wire as counter electrode, and Ag/AgCl as the reference electrode. The electrode material (1 mg) was prepared using 90 wt% sample, 5wt% activated carbon and 5 wt% polytetrafluoroethylene. This mixture was coated on a graphite sheet surface which was dried at 80 °C for 4 hr. The electrochemical tests were performed in 0.5M K_2SO_4 aqueous electrolyte solution at atmospheric temperature.

3. Results and discussion

3.1 Structural and Morphological studies

The X-ray diffraction patterns of CuO annealed at different temperatures are shown in Fig.1. The diffraction peaks matches well with the JCPDS(card no. 05-0661) data for CuO. Moreover, the CuO nanostructures exhibit monoclinic symmetry (C_2/C space group) and lattice

constant values, $a = 0.4684$ nm, $b = 0.3425$ nm and $c = 0.5129$ nm: $\beta = 99.47^\circ$. It is obvious that the intensity of the diffraction peaks increase with the increase of annealing temperature which confirms the occurrence of better crystalline nature at higher annealing temperatures. Further, the absence of any collateral peaks in the XRD pattern indicates the high purity of the prepared CuO samples.

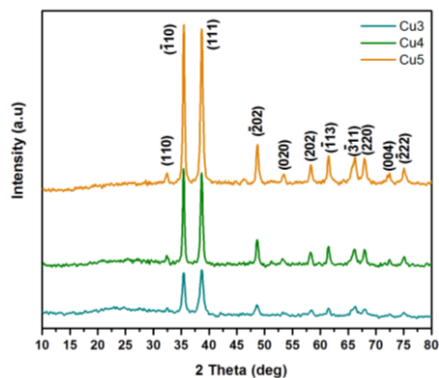


Fig. 1 X-ray diffraction (XRD) pattern of the Cu3, Cu4 and Cu5

The morphological features of CuO nanostructures annealed at different temperatures are evaluated by field emission scanning electron and transmission electron microscopy. Fig. 2 shows the FESEM images of the sample annealed at 300°C, 400°C and 500 °C. The formation of uniform spindle like morphology has been observed for Cu3. Increase in annealing temperature leads to the transformation of spindle like structure and formation of worm like morphology at 400°C and 500°C. Further increase in annealing temperature results in the aggregation of worm like structure. The schematic representation of the formation mechanism is shown in Fig.3.

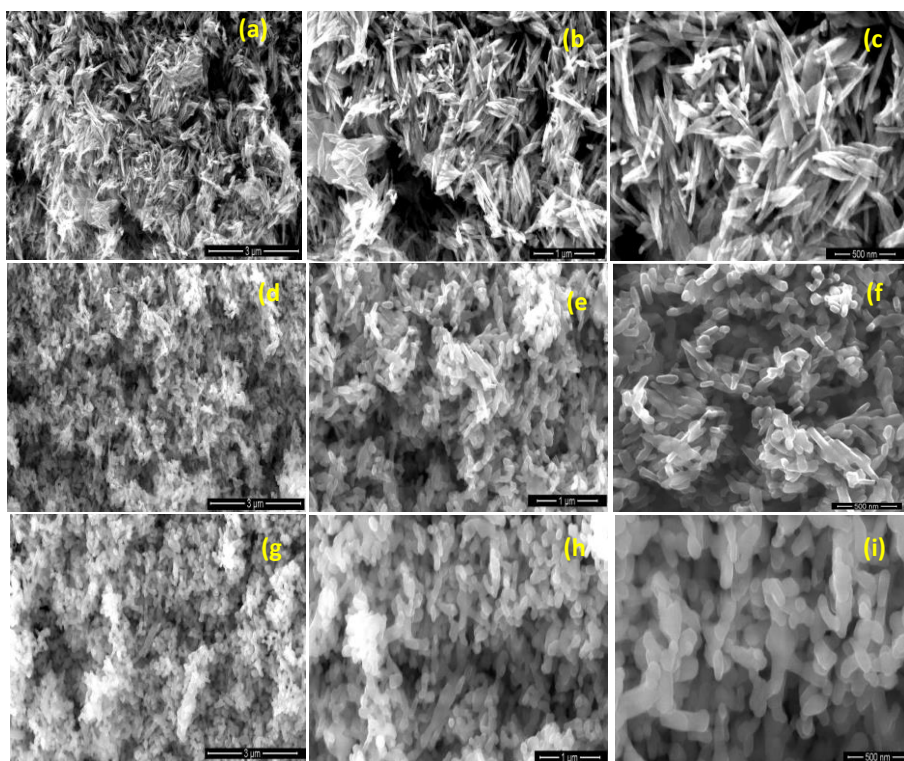


Fig. 2 FESEM images of Cu3 (a,b,c), Cu4 (d,e,f) and Cu5 (g,h,i).

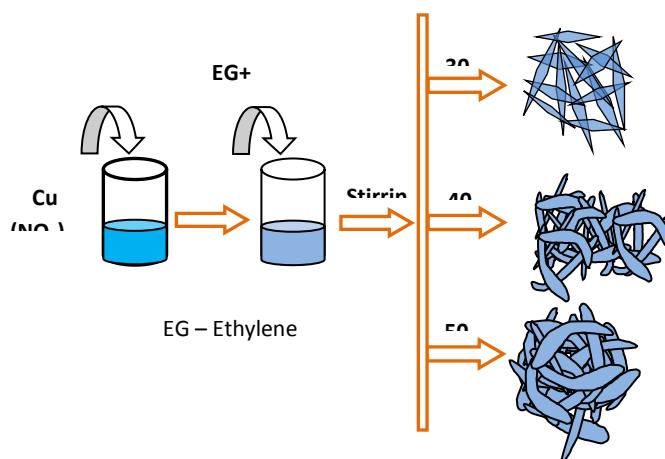


Fig. 3 Schematic illustration of formation mechanism of CuO nanostructures

3.2 Electrochemical Studies

3.2.1 Cyclic voltammetry analysis

To evaluate the electrochemical performance of the CuO nanostructures, the cyclic voltammetry analysis (CV) has been carried out between -0.6 to 0.6 V using 0.5M K_2SO_4 electrolyte.

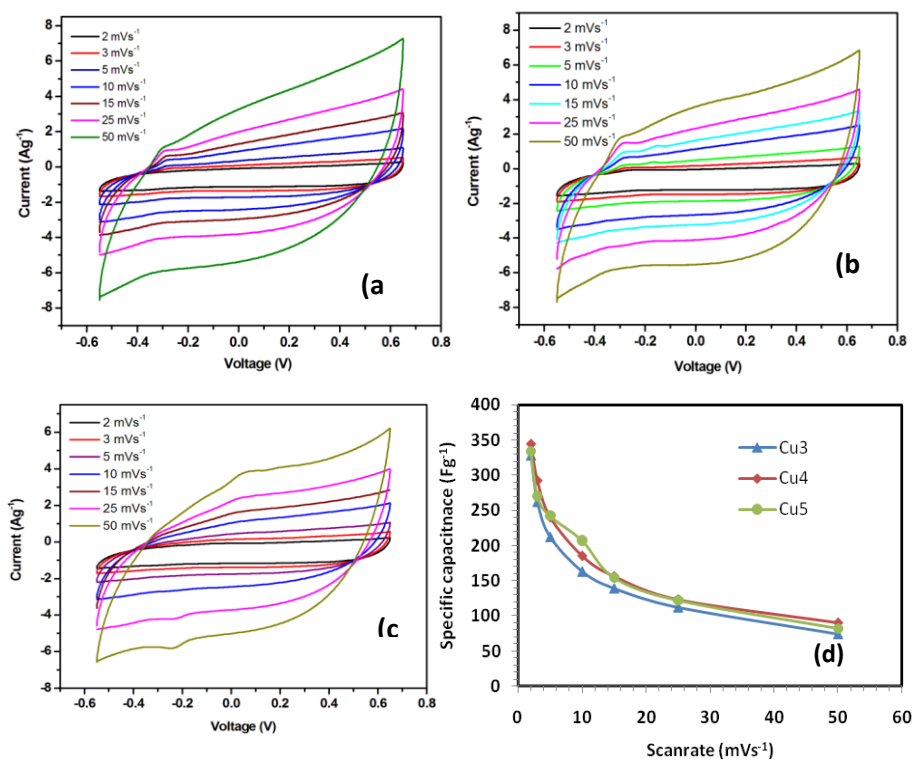


Fig. 4 CV curves of Cu3 (a), Cu4(b) and Cu5(c) at various scan rates and specific capacitance as a function of scan rate (d).

Fig. 4 shows the CV curves of CuO nanostructures annealed at different temperatures at different scan rates. The CV curves of the samples Cu3, Cu4 and Cu5 confirms the presence of redox peaks in their cathodic and respective anodic scan indicates the significant share of pseudocapacitance in the electrochemical process. The specific capacitance of CuO

nanostructures synthesized at different annealing temperatures were estimated using the following equation,

$$C = \frac{i}{\nu \times m} \quad (1)$$

where C (Fg^{-1}) is the specific capacitance, m (mg) is the mass of the active material, i (mA) is the average current and ν (v) is the scan rate. The calculated values of specific capacitance of the samples at 2 mVs^{-1} are 329 Fg^{-1} , 345 Fg^{-1} and 334 Fg^{-1} respectively. The higher capacitance of Cu4 is attributed to the worm like structure which provides additional pathways for electrolyte penetration. Dubal et al., reported the specific capacitance of 178 Fg^{-1} for CuO cauliflowers in the potential window of 0-0.4 V [12]. CuO/Cu(OH)₂ exhibits the specific capacitance of 278 Fg^{-1} between 0 to 0.55 V was reported by Hsu et al., [13]. The CuO nanoworms synthesized as stated beforehand exhibits higher specific capacitance when compared with the aforesaid works. Fig. 4(e) illustrates the variation of specific capacitance with different scan rates for all the three electrodes. The increase of scan rate weakens the specific capacitance significantly due to the inability of electrolyte ions to access the interior parts of the electrode active materials at higher scan rates [14].

3.2.2 Galvanostatic charge discharge analysis

To explore the electrochemical richness of CuO nanostructures and to determine the discharge specific capacitance, the galvanostatic charge–discharge (GCD) measurements were carried out using 0.5 M K₂SO₄. Fig. 5(a) presents the GCD profiles of Cu3, Cu4 and Cu5 at the current density of 0.5 Ag^{-1} . The discharge specific capacitance values are determined from GCD curves based on the following relation,

$$C = \frac{I \times \Delta t}{m \times \Delta v} \quad (2)$$

where I (mA), Δt (s), Δv (V) and m (mg cm^{-2}) are the discharging current, discharge time, potential window and mass loading of the active material in the electrode. The calculated discharge specific capacitance of Cu3, Cu4 and Cu5 electrodes are 235 Fg^{-1} , 298 Fg^{-1} and 268 Fg^{-1} respectively. As expected, due to morphological richness, Cu4 electrode exhibits the higher specific capacitance compared to other electrodes. Further, the decreased specific capacitance for Cu5 is attributed to the increase in the crystalline nature of the material. The formation of compact crystalline may decrease the ion movement. In addition, Fig.5 (b, c, d) presents the GCD profiles of Cu3, Cu4 and Cu5 electrodes at different current rates. The variation of specific capacitance with different current densities is shown in Fig. 5e. Zhang et al., reported [15] the specific capacitance of 130 Fg^{-1} at 1 Ag^{-1} for CuO nanobelts. In the present work CuO nanoworms exhibit higher specific capacitance, when compared with aforesaid work.

The cyclic lives of the CuO electrodes are investigated by carrying out the continuous charge-discharge test at a current density of 10 Ag^{-1} . Fig. 6 presents the cyclic stability test of Cu3, Cu4 and Cu5 up to 1500 cycles. The Cu4 electrode show higher percentage (99%) of capacitance retention up to 1500 cycles compared to Cu3 (84%) and Cu5 (95%). When compared to the 91% stability up to 1000 cycles as verified by Prasad et al., [16] for CuO nanoparticles and 90.6% stability up to 500 cycles as confirmed by Hang et al., [17] for hierarchical CuO nanostructures, the Cu4 electrode in our study has shown higher cyclic stability.

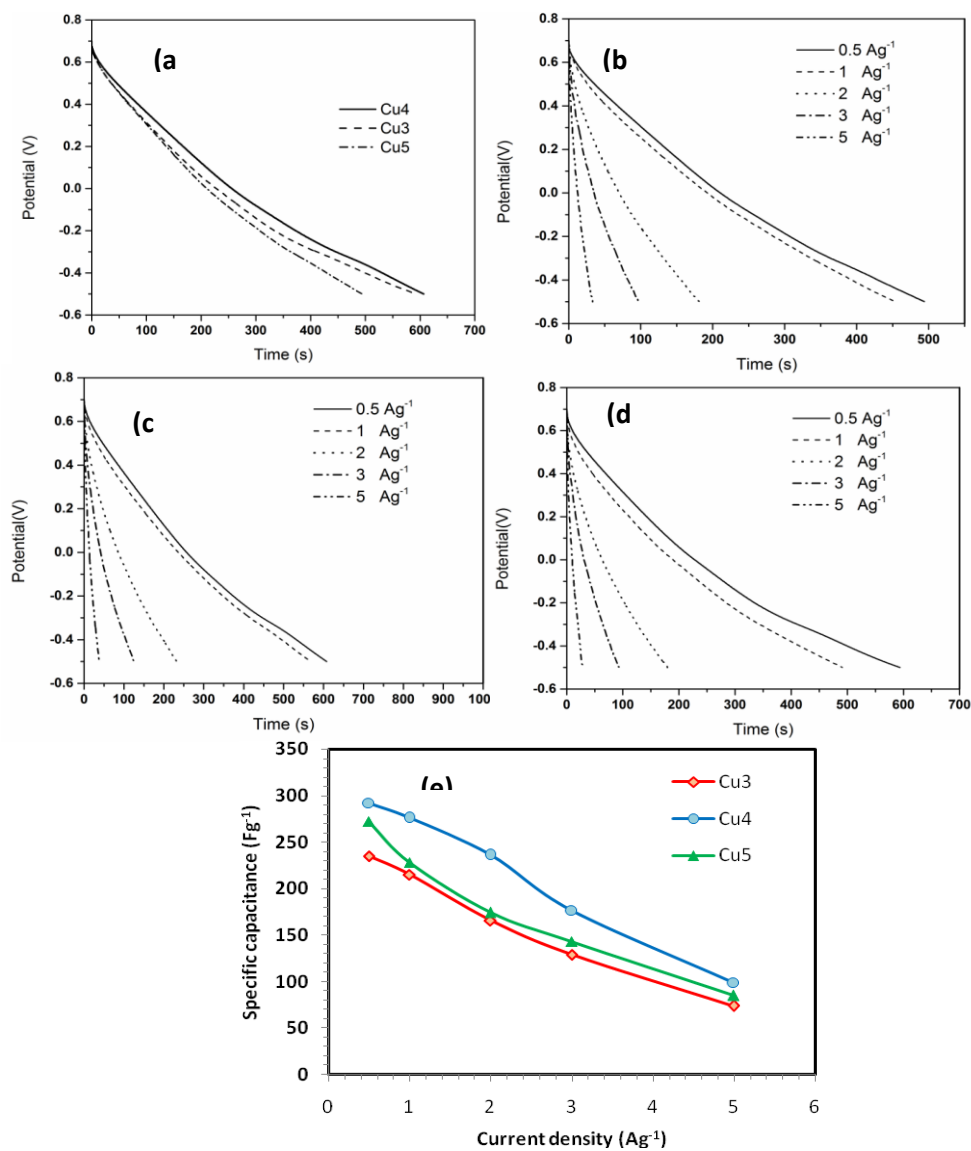


Fig. 5. Discharge curves of Cu3, Cu4 and Cu5 at a current density of 0.5 Ag^{-1} (a), Discharge curves of Cu3 (b), Cu4(c) and Cu5 (d) at various current densities and Variation of specific capacitance with different current densities (e).

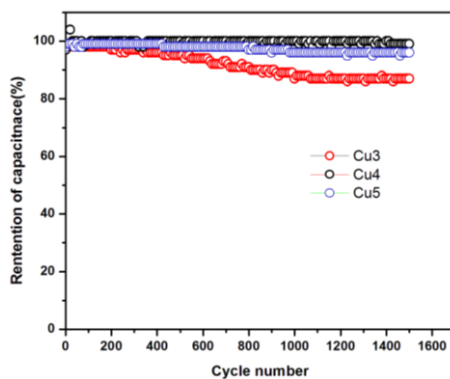


Fig. 6 Cyclic stability of Cu3, Cu4 and Cu5

3.2.3 Electrochemical impedance analysis

Additionally, the electrochemical impedance spectroscopy (EIS) measurements were performed to attain the details regarding the conductive nature of the CuO nanostructures. Fig.7 shows the Nyquist plot of Cu3, Cu4 and Cu5 electrodes. These plots have semicircle arc at high frequency region which represent the charge transfer resistance (R_{ct}). The inclined straight line at low frequency region specifies the lower diffusion resistance. The R_{ct} values of Cu3, Cu4 and Cu5 electrodes are 9.8 Ω , 3.3 Ω and 3.6 Ω respectively. The lower value R_{ct} of Cu4 electrode leads to higher capacitance when compared to other electrodes.

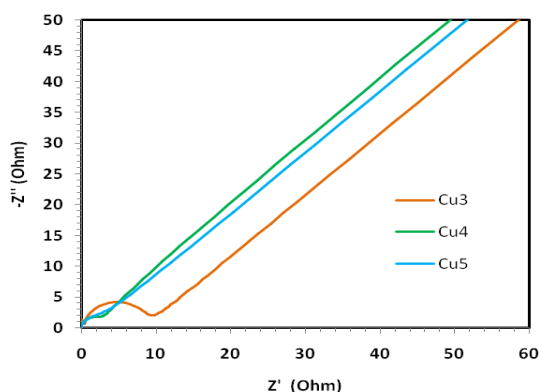


Fig. 7 Nyquist plots for the Cu3, Cu4 and Cu5

3.2.4 Fabrication and analysis of Asymmetric supercapacitor device

An asymmetric supercapacitor device (ASC) has been fabricated using the sample Cu4 as anode and activated carbon as cathode materials. Fig 8(a) presents the cyclic voltammograms of Cu4 //AC asymmetric supercapacitor at different sweep rates. The discharge profiles at different current densities are shown in (Fig. 8b). The calculated specific capacitance values are 47 Fg^{-1} , 43 Fg^{-1} , 30 Fg^{-1} and 23 Fg^{-1} at the current densities of 1, 2, 3 and 4 Ag^{-1} respectively. The device exhibits an energy density of 6.5 Whkg^{-1} with the power density of 249 Wkg^{-1} . Employing EIS measurements, the electrochemical behaviour of Cu4 //AC asymmetric device was analysed and presented using the Nyquist plot (Fig. 8c). The observed charge transfer resistance (R_{ct}) is 68 Ω . This asymmetric system exhibited capacitance retention of 81% (Fig.9d) after 100 cycles at a current density of 10 Ag^{-1} .

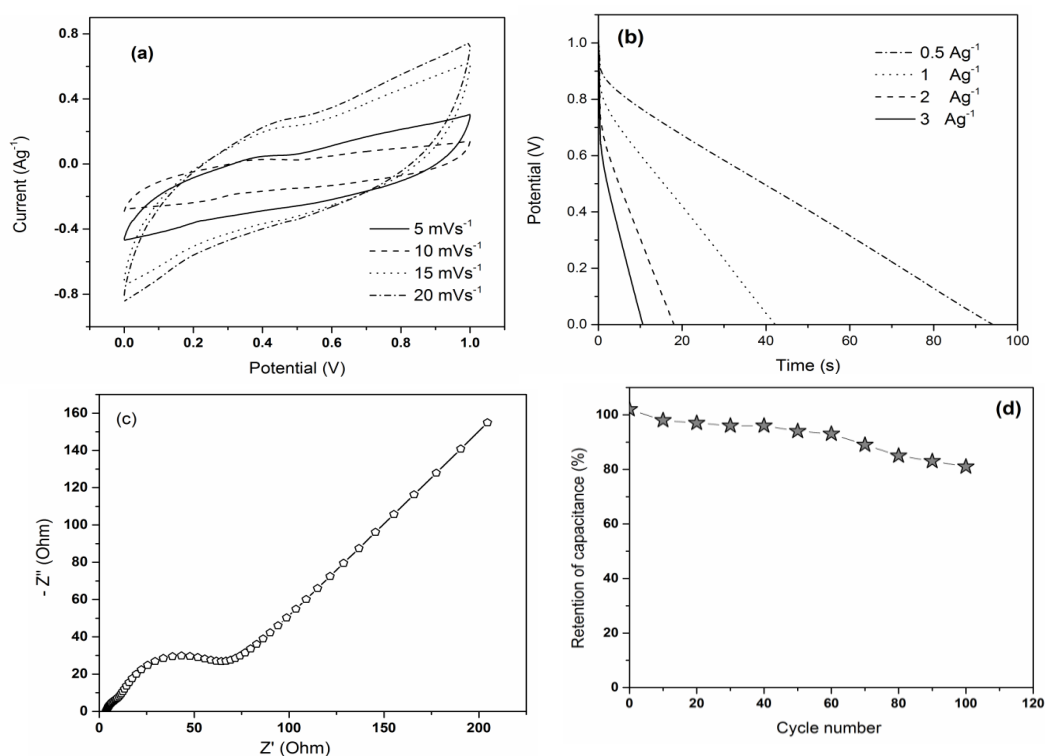


Fig. 8 Cu₄//AC asymmetric device performance. (a) CV curves at various scan rates. (b) Discharge curves at different current densities (c) Nyquist plots (d) Cyclic stability

4. Conclusion

Simple and cost effective method has been used to synthesis CuO nanospindles and nanoworms. The XRD analysis shows the increase in crystalline nature with increase in annealing temperature. The formation of nanoworm like structure enhances the electrochemical properties significantly. CuO annealed at 400°C reveals higher specific capacitance (345 Fg⁻¹), better cycling stability (99% up to 1500 cycles) and lower charge transfer resistance (3.3 Ω). The asymmetric device discloses the maximum specific capacitance of 47 Fg⁻¹ at a current density of 1 Ag⁻¹.

References

- [1] P.Simon, Y.Gogotsi, Nat. Mater. **7**, 845 (2008).
- [2] Y.Z. Su, K. Xiao, N. Li, Z.Q. Liu, S.Z. Qiao, J. Mater. Chem. A, **2**, 13845 (2014).
- [3] C. F. Zhang, Y. Xie, M. Zhao, A. E. Pentecost, Z. Ling, J. Wang, D. Long, L. Ling, W. Qiao, ACS Appl. Mater. Interfaces **6**, 9751 (2014).
- [4] X. Su, X. Yang, L. Yu, G. Cheng, H. Zhang, T. Lin, F. H. Zhao, Cryst. Eng. Comm, **17**, 5970 (2015).
- [5] G. Ye, Y. Gong, K. Keyshar, E. A. M. Husain, G. Brunetto, S. Yang, R. Vajtai, P. M. Ajayan, Part. Syst. Charact., **32**, 817 (2015).
- [6] K. Anandan, V. Rajendran, Mater.Sci.Semi. Proces. **14**, 43 (2011).
- [7] X. Lang, A. Hirata, T. Fujita and M. Chen, Nat. Nanotechnol. **6**, 232 (2011).
- [8] C. Guan, J. Liu, C. Cheng, H. Li, X. Li, W. Zhou, H. Zhang and H.J. Fan, Energy Environ. Sci., **4**, 4496 (2011).
- [9] M. F. Cain, R. P. Hughes, D. S. Glueck, J. A. Golen, C. E. Moore, A. L. Rheingold, Inorg. Chem. **49**, 7650 (2010).
- [10] R. K. Bedi, I. Singh, ACS Appl. Mater. Interfaces, **2**, 1361 (2010).

- [11] N. D. Hoa, N. Van Quy, H. Jung, D. Kim, H. Kim, S.K. Hong, **146**, 266 (2010) .
- [12] D. P. Dubal, G. S. Gund, C. D.Lokhande, R.Holze, Mater. Research. Bull.**48**, 923 (2013).
- [13] Y.K. Hsu, Y.C. Chen, Y.G. Lin, L.C. Chen, K.H. Chen, Chem. Commun. **21**, 324 (2011).
- [14] G. Wee, H. Z. Soh, Y. L. Cheah, S. G. Mhaisalkar, M. Srinivasan, J. Mater. Chem., **20**, 6720 (2010).
- [15] X. Zhang, W. Shi, J. Zhu, D. J. Kharistal, W.Zhao, B.Lalia, H.H.Hng and Q.Yan ACS Nano **5**, 2013 (2011).
- [16] K. P. S. Prasad, D. S Dhawale 1, T. Sivakumar, S. S Al Deyab, J. S. M. Zaidi, K. Arigal, A.Vinu, Sci. Technol. Adv. Mater. **12**, 44602 (2011).
- [17] Y. X. Zhang, M. Huang, F. Li, Z.Q. Wen, Int. J. Electrochem. Sci., **8**, 8645 (2013).